

## Quantifying and mapping cooling services of multiple ecosystems

Chae Yeon Park <sup>a</sup>, Yoon Sun Park <sup>b</sup>, Ho Gul Kim <sup>c</sup>, Seok Hwan Yun <sup>d</sup>, Choong-Ki Kim <sup>b,\*</sup>

<sup>a</sup> Social Systems Division, National Institute for Environmental Studies, 305-8506, 16-2 Onogawa, Tsukuba, Ibaraki, Japan

<sup>b</sup> Division for Natural Environment, Korea Environment Institute (KEI), Sejong, 30147, Republic of Korea

<sup>c</sup> Dept. of Human and Environment Design, Cheongju University, Cheongju, Republic of Korea

<sup>d</sup> Interdisciplinary Program in Landscape Architecture, Seoul National University, Seoul, Republic of Korea



### ARTICLE INFO

#### Keywords:

Urban heat  
Green spaces  
Water bodies  
Cooling effect  
Sensible heat flux  
Energy saving potential

### ABSTRACT

The higher heat load in urban areas than that in rural areas increases the heat stress of citizens and cooling load. Ecosystem-based planning can be a cost-effective solution for cooling cities. In this study, we quantified and mapped the cooling services of multiple ecosystems based on sensible heat mitigation effects and their energy saving potential during the hottest time of the day. Forests, grassland, water bodies, and swamps were considered in this study, and we identified the most efficient ecosystems in the study area with low cooling services. Water bodies exhibited the highest cooling service by mitigating the sensible heat flux by up to 250 W/m<sup>2</sup>. However, forests made the greatest contribution due to their higher area ratio than that of water. These ecosystems can reduce the energy required for air-conditioning during the hottest time of the day by approximately 0.15 kWh/m<sup>2</sup>. The cooling service quantifying and mapping methods proposed in this study can help urban planners to develop more sustainable and resilient cities that can more efficiently incorporate ecosystem-based cooling services.

### 1. Introduction

Urban areas have fewer green spaces and water bodies that can provide evaporative cooling effects than rural areas (Taha, 1997), and they have a larger proportion of impervious surfaces that absorb more solar radiation and store excess heat (Li et al., 2015). This increases the upward sensible heat flux, thereby increasing the canopy layer air temperature (Erell et al., 2014). Increased urban heat raises heat stress in humans and affects heat-related mortality (Thorsson et al., 2014), and tends to result in an increased cooling load (Davies et al., 2008). Additionally, climate change leads to more frequent and intense extreme heat events, with severe consequences (Matthews et al., 2017). To reduce the impact of urban heat on building energy and improve human health, urban heat mitigation is a critical issue for governments, businesses, and communities (Bolitho & Miller, 2017).

The cooling effect of ecosystems may be the key to reducing the air temperature and increasing urban resilience against future heat events. Ecosystem services refer to the benefits derived from ecosystems (Martinez-Harms & Balvanera, 2012), one of which involves regulating the local climate by modifying the temperature, wind, radiation, and precipitation (Burkhard et al., 2012). Ecosystem-based planning is a

flexible and cost-effective approach to reducing urban heat (Augusto et al., 2020; Munang et al., 2013) that not only produces cooling effects in urban areas, but also provides other benefits, such as pollution reduction (Norton et al., 2015) and socioeconomic development (Peng et al., 2020).

Green areas, such as urban parks and trees along streets, provide cooling through shade and evapotranspiration (Zardo et al., 2017). Trees provide shade and reflect incoming shortwave radiation, reducing the heat load on urban surfaces and building cooling loads (Akbari & Taha, 1992; Arsmo et al., 2013). Vegetation in urban areas releases latent heat flux through evapotranspiration (Grimmond & Oke, 1991). Napoli et al. (2016) observed that trees reduced surface temperatures by up to 22.8 °C due to the combined effects of shade and evapotranspiration, and grass reduced surface temperatures by up to 9.4 °C. The cooling effect of a green area depends on its size, type, and structure (Park et al., 2017).

Water bodies are another important ecosystem in urban areas, as they can be used in climate-sensitive urban design to lower temperatures and improve human thermal comfort (Coutts et al., 2012). Wu and Zhang (2019) demonstrated that water bodies reduced the surface temperature during the daytime by up to 3 °C over an area of up to 800

\* Corresponding author

E-mail address: [ckkim@kei.re.kr](mailto:ckkim@kei.re.kr) (C.-K. Kim).

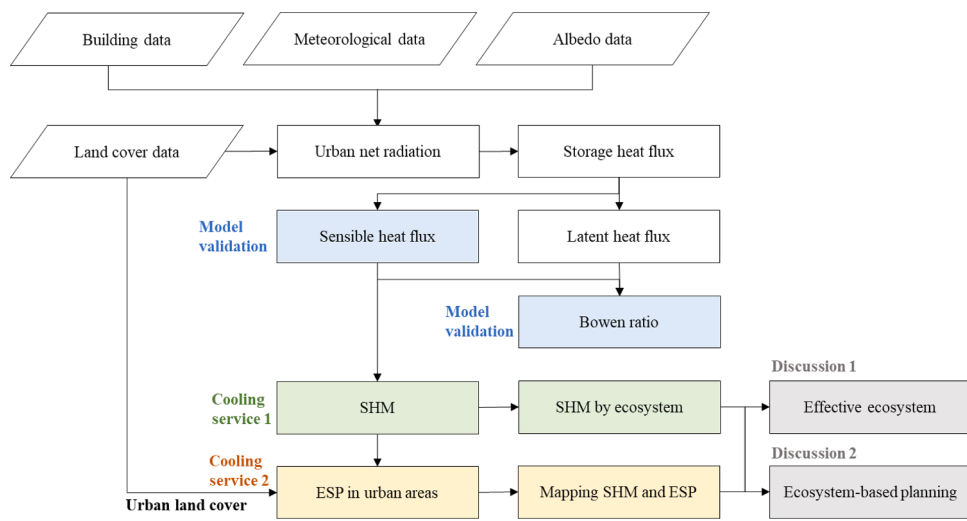


**Fig. 1.** Study flow chart.

m. This is because water bodies generate latent heat flux via evaporation, and this cooling effect increases until 2–5 pm following the build-up of water surface energy (Zuo et al., 2016). Therefore, water bodies can reduce the urban heat flux during the hottest period of the day.

Previous studies have estimated the cooling effects of green spaces and water bodies by measuring the air temperature or land surface temperature (LST) at neighborhood- or city-scales. For neighborhood-scale measurement, the air temperature was retrieved from fixed meteorological stations, with limited spatial coverage. Recent studies have utilized the mobile traverse method to cover wider areas in a city and compared the air temperatures of different land-cover types. For example, the mobile traverse method was used to determine that a 10% increase in vegetation coverage cooled the air temperature by 0.05–0.15 °C (Yan et al., 2020), and the cooling effect was greatest when the vegetation cover exceeded 40% (Ziter et al., 2019). However, mobile measurement methods limited in that they are highly time-consuming and have low spatial coverage; thus, it is difficult to measure the city-wide cooling effects. Therefore, many researchers have used the LST to measure cooling effects at the city-scale by using remote sensing data. The LST is an effective indicator for determining the (1) range and magnitude of the land surface cooling effect (i.e., cooling extent and intensity) (Du et al., 2016; Sun et al., 2012; Wu & Zhang, 2019; Ziter et al., 2019) and (2) effective composition and configuration of an ecosystem (Hou & Estoque, 2020; Masoudi et al., 2021; Tan et al., 2021). However, it is difficult to analyze the generation mechanism and energy change in urban areas using the LST, and the LST is limited by low temporal resolutions (Yu et al., 2020).

Modeling the urban energy balance can overcome the limitations of the LST. Many previous studies have developed and validated heat generation and mitigation mechanisms (Bruse, 1999; Grimmond et al., 1991; Grimmond & Oke, 1991, 2002; Järvi et al., 2011). ENVI-met is predominately used to estimate neighborhood-scale cooling effects (Jacobs et al., 2020; Ouyang et al., 2020; Zöhl et al., 2016). Researchers have used the urban energy model to explore the city-scale cooling effect based on land-cover type, which calculates heat mitigation effects based on changes in radiative forcing, surface reflection, and biophysical (evapotranspiration) heat exchanges (Augusto et al., 2020; Lee et al., 2011; Luyssaert et al., 2014). This heating mechanism requires us to explicitly analyze the cooling effects of ecosystems, regardless of their temporal or spatial extent.

Urban energy balance modeling has other advantages in ecosystem service studies. First, it can be directly converted into the energy saving potential (ESP) (Xu et al., 2019; Zhang et al., 2014), which can reflect

the monetary value of ecosystem services. Kumari et al. (2020) estimated the effects of LST on energy consumption using statistical analysis, and areas with high vegetation coverage were found to reduce the LST and reduce annual energy consumption by 19.5 MWh. However, this was a case study for Delhi, India, and it is difficult to generalize the energy saving results to other cities. Second, energy balance modeling allows us to quantify the cooling effects of multiple ecosystems. Many previous studies have focused on identifying the cooling effect of a single ecosystem (Foudi et al., 2017; Monteiro et al., 2016; Moss et al., 2019; Sun et al., 2012; Wu & Zhang, 2019; Zhang et al., 2014). Urban heat mapping considers diverse land-cover types (such as tree cover, grass, and water) (Augusto et al., 2020), that can be used to generate and compare the cooling effects (i.e., ESP) of different ecosystems. However, studies modeling ecosystem cooling effects using the urban energy balance and data with high spatial resolution (similar to the LST method) remain limited.

In this study, we explore the sensible heat mitigation (SHM) and ESP services of multiple ecosystems at the city scale based on urban energy balance modeling. This method allows us to observe the spatially heterogeneous cooling effect in urban areas. This study investigates the following research questions. (1) Which ecosystem exhibits the most effective cooling effect in urban areas? (2) Where are the areas with lower cooling effects? The comparison of multiple ecosystems can aid in improving the ecosystem-based planning efficiency for cooling cities, and the spatial distribution map can identify priority areas for future conservation or renovation.

## 2. Materials and methods

We defined the cooling services of multiple ecosystems as the amounts of SHM and ESP (Fig. 1). To estimate the sensible heat flux, we used a local-scale urban heat storage (Grimmond & Oke, 2002), energy partitioning (De Bruin & Holtslag, 1982), and urban canopy shortwave and longwave radiation transfer methods using three-dimensional urban data (Kwon et al., 2019). These methods require simple data and the heat flux mechanisms are applied according to land-cover type, which is appropriate for estimating the cooling services of multiple ecosystems within a city. Although the urban radiation model was validated using the measured radiation in South Korea (Kwon et al., 2019), we also compared the simulated sensible heat flux and Bowen ratio (ratio of the sensible heat exchange to latent heat exchange) to those of previous studies (Douglas et al., 2009a; Kuang et al., 2014; Kuang et al., 2017) in order to validate the land-cover parameters used in the model. Additionally, we calculated the hourly variation in sensible heat and

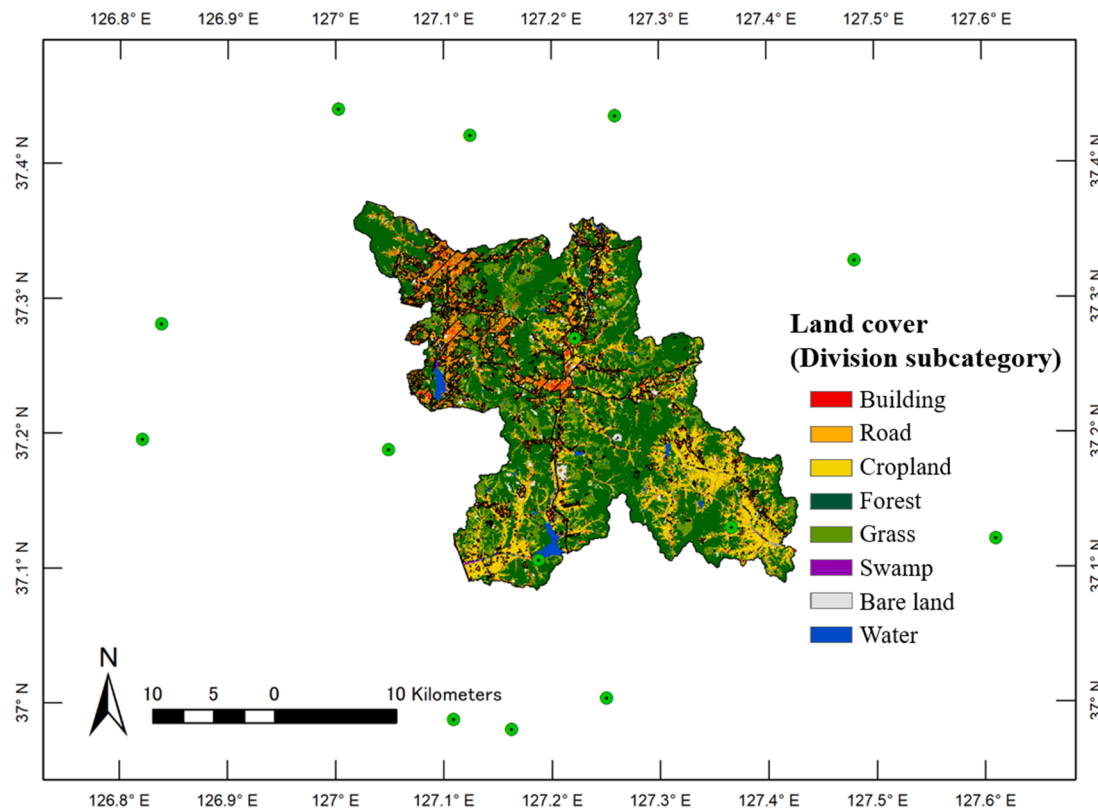


**Fig. 2.** Study site and land-cover types. Land-cover types and urban areas (slashed area) were derived from the national land-cover data subcategories and main categories, respectively. Green points indicate the AWS locations.

compared it to that of previous studies. We also compared the SHM of different ecosystems to identify the most effective ecosystem for city cooling. We created scatter plots between each ecosystem area ratio and SHM, allowing us to identify the increased ratio of SHM when increasing the area ratio of each ecosystem and identified the contribution of each ecosystem to the total cooling service. For the second ecosystem service indicator, we calculated the ESP within the urban area. Based on the results, we discussed (1) the effects of forest, grassland, water body, and swamp ecosystems on cooling and (2) how to use cooling service mapping for ecosystem-based planning.

### 2.1. Study site

This study focuses on Yongin-si, South Korea, due to its unsustainable development and lack of ecosystem services (Fig. 2). Yongin-si is the fourth largest city in the metropolitan area of South Korea, with a population of over one million. Yongin-si has been expanded since 2000 without a sustainable development plan (Nam, 2009). Many high-density residential buildings have been constructed in forest areas (Kim, 2009), which has led to ecosystem destruction. Urban areas in Yongin-si exhibit few green spaces and high heat risk. In contrast, there are undeveloped areas in Yongin-si with high forest ratios, allowing us to compare the differences in ecosystem service between these two types of areas.

### 2.2. Input data

We quantified and mapped sensible heat flux using data from national agencies and satellites. There were four types of input data: land-cover, meteorological, building, and albedo data. We targeted daytime hours from 10:00 to 16:00 (local time) during summer (June–August) 2019 as the outdoor heat stress is highest during this period (Lee et al., 2013).

The land-cover and ecosystem types were related in this study. Many studies have demonstrated that green areas and water bodies exhibit cooling effects (Hou & Estoque, 2020; Tan et al., 2021; Venevsky et al., 2019; Ziter et al., 2019). Based on the subcategory of land-cover classification, green areas can be divided into forest and grassland, which have different cooling effects. Water bodies are divided into water and swamps, which also have different evaporation characteristics. Other land-cover types are also considered to calculate the sensible heat flux, including cropland, buildings, roads, and bare land. Here, we defined built-up areas as a combination of buildings and roads. We extracted the land cover types (forest, grassland, swamp, water, cropland, buildings, roads, and bare land) from the subcategory land-cover map produced by the Korea Ministry of Environment (MOE, 2019), and were incorporated as area ratios in a grid.

We obtained air temperature and relative humidity data from fourteen automatic weather stations (AWSs) of the Korea Meteorological Administration (KMA, 2020) located within or surrounding Yongin-si (Fig. 2). We averaged the data for 92 days (June–August 2019) in order to determine the average summer hourly air temperature from 14 stations and relative humidity from 12 stations, as two were unavailable, and then interpolated the point values by inverse distance weighting interpolation in QGIS (version 3.12.2).

Building data are important for estimating the sensible heat flux, as the building shade and sky view factor (visible portion of the sky; SVF) affect the radiation transfer in the urban canopy. A low-SVF area with a high building shade ratio reduces the areal exposure to shortwave radiation (Lai et al., 2019). We used building data from the Korea National Spatial Data Infrastructure Portal (KNSPDIP, 2020), we estimated building elevation model. Then, we calculated building shade using the hillshade tool of ArcGIS (version 10.7, ESRI) hourly at a 2-m scale. This tool calculates whether the cell falls in a shadow or not by considering illumination direction, and the elevation of cell's eight neighbors (Burrough & McDonnell, 1998). We calculated the SVF using SAGA-GIS

**Table 1**

Sensible heat flux parameters by land-cover type.

Parameter	Albedo*	Latent heat flux	Storage heat flux			References for $\alpha$	References for $\beta$ , $\gamma$ , and $\delta$
	$alb$	$\alpha$	$\beta$	$\gamma$	$\delta$		
Water	0.093	1.3	0.5	0.21	-39.1	Hanna & Chang (1992b)	Roberts et al. (2006)
Swamp	0.125	1.2	0.5	0.21	-39.1		Roberts et al. (2006)
Forest	0.095	1	0.11	-0.11	-12.3		Grimmond et al. (1991)
Grass	0.118	0.8	0.34	0.31	-31		Grimmond & Oke (2002)
Crop	0.133	0.8	0.34	0.31	-31		
Bare land	0.132	0.5	0.38	0.56	-27.3		Grimmond et al. (1991)
Road	0.122	0.2	0.7	0.33	-38		Grimmond & Oke (2002)
Building	0.126	0.2	0.13	0.45	-9		

\*Albedo by land-cover type was calculated using 2019 albedo data.

(version 2.1.4) at a 2-m scale. SVF calculation is based on horizontal angles in different azimuth directions of the full circle around each grid cell (Böhner & Antonić, 2009). The building shade area ratio and mean SVF value were incorporated in a grid.

Finally, the albedo was calculated using 2019 June–August Landsat 8 Collection 1 Tier 1 calibrated top-of-atmosphere reflectance images with cloud coverage of less than 10%. We calculated the mean albedo in the study area by land-cover type (Table 1).

All input variables were converted to grid-type variables. The grid resolution should be sufficient to capture all relevant effects of the biophysical processes (Perrings et al., 2011). Here, 100 × 100 m was sufficient to contain all relevant surface information for urban energy balance modeling (Grimmond et al., 1991).

### 2.3. Cooling service calculation

Sensible heat flux plays a critical role in land–atmosphere interaction (Zhuang et al., 2016). Air temperature changes are accompanied by energy variation, particularly a reduction in the sensible heat fluxes (Augusto et al., 2020; Wu & Chen, 2017). The sensible heat flux detects thermal-related mortality more accurately than the air temperature in South Korea (Kwon et al., 2020). The SHM by an individual ecosystem service  $i$  ( $SHM_i$ ) is the reduction in heat flux by the individual ecosystem area ratio compared to the built-up land-cover (50% roads and 50% buildings) (Eq. 1).

$$SHM_i = Qh_{i \rightarrow b} - Qh_i (\text{W/m}^2) \quad (\text{Eq. 1})$$

where  $Qh_{i \rightarrow b}$  is the sensible heat flux with a change in ecosystem ( $i$ ) to built-up areas, and  $Qh_i$  is the sensible heat flux with the area ratio of ecosystem ( $i$ ).

According to the energy balance equation, the sensible heat flux is given by:

$$Qh = Qnet - Qs - Ql (\text{W/m}^2) \quad (\text{Eq. 2})$$

where  $Qnet$  is the urban net radiation,  $Qs$  is the storage heat flux, and  $Ql$  is the latent heat flux. We calculated the net radiation flux using the method developed by Kwon et al. (2019) to map the spatial distribution of heat within a city using building data. This method was based on the shortwave and longwave radiation model (Allen et al., 1998; Loridan et al., 2011). The primary radiation-reducing behavior of the ecosystem involves the prevention of incoming shortwave radiation by forming shade and radiation trapping in low-SVF areas by reflecting radiation off of the surfaces. Forests exhibit different radiation transfer behaviors to grasslands and water bodies due to the presence of trees, which prevent the radiant heat flux from reaching the ground by creating shade (Napoli et al., 2016). As the shade ratio in the forests cannot be observed, we assumed that the trees in the forest were at the same height and that the shade ratio was one below the trees and zero above the canopy level ( $shd=0.5$ ) (Park et al., 2021). The net radiation is the sum of the shortwave and longwave radiation remaining in the urban canyon (Eq. 3).

$$Qnet = SW_{down} + LW_{down} - SW_{up} - LW_{up}, (\text{W/m}^2) \quad (\text{Eq. 3})$$

where  $SW_{down}$  and  $LW_{down}$  are the urban downward shortwave and longwave radiation, and  $SW_{up}$  and  $LW_{up}$  are the urban upward shortwave and longwave radiation, respectively. Each radiation component can be calculated using Eqs. 4–10.

$$\begin{aligned} SW_{down} = & ((1 - shd) \times SW_{dir} + SVF \times S_{dif}) + (1 - SVF) \times (1 - shd) \\ & \times (SW_{dir} + SW_{dif}) \times alb_{building} \end{aligned} \quad (\text{Eq. 4})$$

where  $shd$  is the shade ratio,  $SW_{dir}$  is the directly downward shortwave radiation,  $S_{dif}$  is the diffused downward shortwave radiation, and  $alb$  is the albedo. We used a value of 0.14 for  $alb_{building}$ .

$$SW_{dif} = SW_{sky} (0.3 + 0.7 \times Fcloud^2), \quad SW_{dir} = SW_{sky} - SW_{dif} \quad (\text{Eq. 5})$$

$$SW_{sky} = (0.75 \times SW_{ext}) \times (1 - 0.75 \times Fcloud^{3.4}) \quad (\text{Eq. 6})$$

where  $SW_{sky}$  is the downward shortwave radiation from the sky, and  $SW_{ext}$  is the extraterrestrial radiation, which is described by Allen et al. (1998).  $Fcloud$  is the cloud fraction that can be calculated using the nonlinear regression of the relative humidity ( $RH$ ) and air temperature ( $T_{a(^\circ C)}$ ) (Eq. 7) (Loridan et al., 2011).

$$Fcloud = 0.185 (\exp \{ (0.015 + 1.9 \times 10^{-4} \times T_{a(^\circ C)}) \times RH \} - 1) \quad (\text{Eq. 7})$$

The upward shortwave radiation is the reflection depending on the albedo ( $alb$ ) (Eq. 8).

$$SW_{up} = SW_{down} \times alb \quad (\text{Eq. 8})$$

$$\begin{aligned} LW_{down} = & SVF \times LW_{sky} + (1 - SVF) \times (LW_{sky} + a \times (SW_{dir} + SW_{dif})) \\ & \times (1 - alb_{building}) \end{aligned} \quad (\text{Eq. 9})$$

where  $LW_{sky}$  is the downward longwave radiation from the sky, which was calculated using the air temperature and cloud fraction, and  $a$  is a constant for converting shortwave radiation to longwave radiation (0.23); more detailed information can be obtained from Loridan et al. (2011).

$$LW_{up} = \varepsilon \sigma \times T_{air(K)}^4 + 0.08 \times shd \times (1 - alb) + (1 - \varepsilon) \times LW_{down} \quad (\text{Eq. 10})$$

where  $\varepsilon$  is the emissivity (0.92), and  $\sigma$  is Stefan's constant ( $5.670367 \times 10^{-8}$ ).

The forest, grassland, water body, and swamp land-cover types exhibited different latent and storage heat flux generation behaviors to impervious areas such as asphalt and concrete. An object urban heat storage model was used to estimate the storage heat flux (Grimmond et al., 1991), which determines different storage heat fluxes based on land-cover as a function of net radiation, rate of change of net radiation,

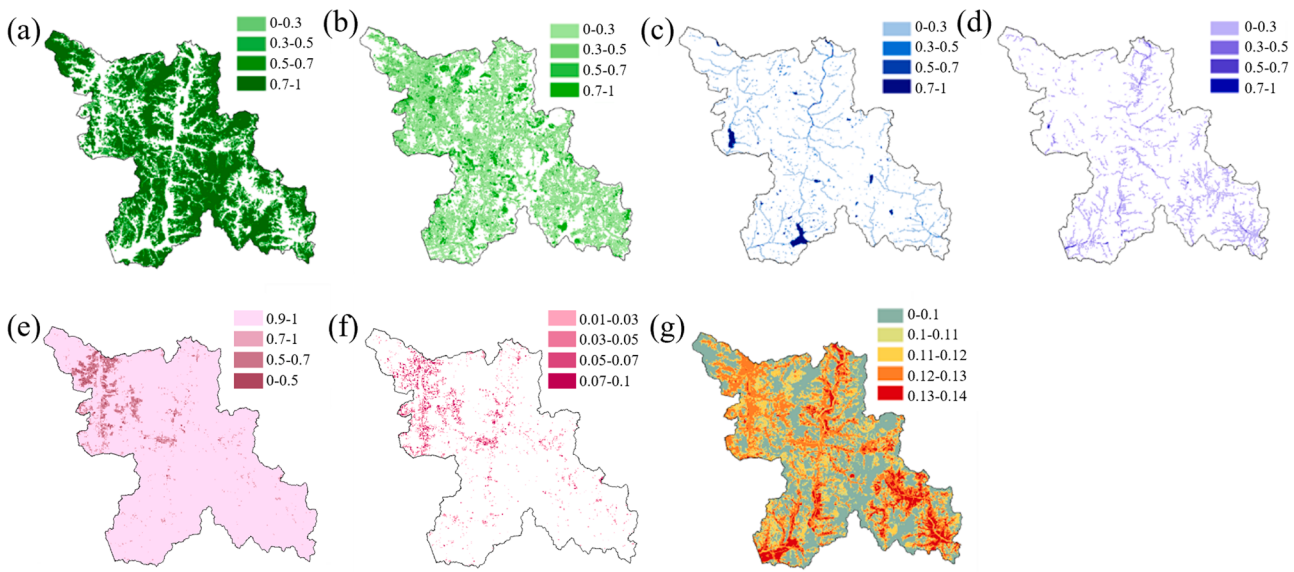


**Fig. 3.** Spatial distributions of the ecosystem area ratios for (a) forest, (b) grass, (c) water, and (d) swamp land-cover types. (e) Mean SVF value, (f) building shade area ratio, and (g) mean albedo.

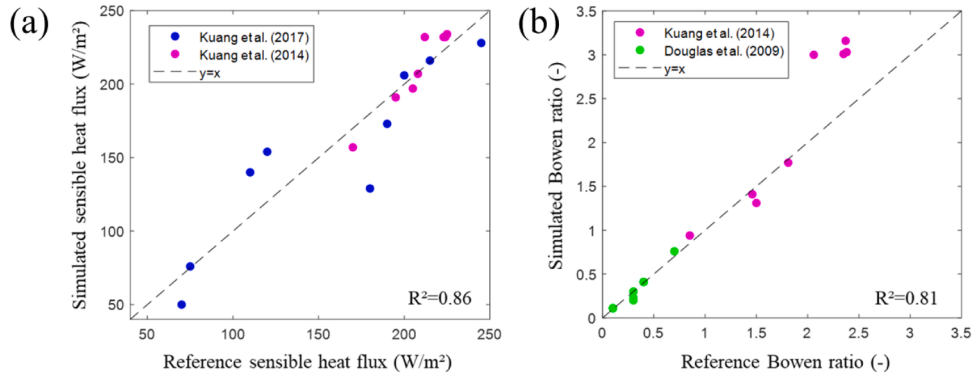


**Fig. 4.** Comparison of the simulated and referenced (a) sensible heat fluxes and (b) Bowen ratios. The data used for urban heat flux simulation are described in Appendix A.

and empirical parameters ( $\beta$ ,  $\gamma$ , and  $\delta$ ) (Eq. 11).

$$Q_s = \beta Q_{net} + \gamma \frac{\partial Q_{net}}{\partial t} + \delta \quad (\text{Eq. 11})$$

where  $\beta$  and  $\delta$  are the coefficients for the relationship between the storage heat flux and net radiation. A positive  $\gamma$  value indicates a peak in the storage heat flux prior to a peak in the net radiation (Grimmond et al., 1991). These empirical parameters were obtained for each land-cover type from Grimmond et al. (1991), Grimmond and Oke (2002), and Roberts et al. (2006) (Table 1).

Green areas can absorb latent heat via evapotranspiration during the summer (Zhang et al., 2014). When water bodies become warmer than the surrounding surface, latent heat cooling reduces the sensible heat flux due to evaporation (Saaroni & Ziv, 2003). Here, the latent heat flux estimations of green areas and water bodies were based on a simple parameterization of the surface fluxes conducted using the Penman-Monteith concept (De Bruin & Holtslag, 1982). The latent heat flux was determined from the saturation vapor pressure temperature curve ( $s$ ), psychrometric constant ( $r$ ), and empirical parameter ( $\alpha$ ), which was related to the moisture status of the surface (Grimmond & Oke, 2002) (Eq. 12); parameter  $\alpha$  was selected for analysis based on Hanna and Chang (1992) (Table 1).

$$Ql = \frac{\alpha}{1 + (r/s)} (Q_{net} - Q_s) + 20 \quad (\text{Eq. 12})$$

The remaining heat flux is the sensible heat flux (Eq. 13).

$$Qh = \frac{(1 - \alpha) + r/s}{1 + (r/s)} (Q_{net} - Q_s) - 20 \quad (\text{Eq. 13})$$

We used the ESP to quantify the cooling service in urban areas where people use air conditioners. Higher heat stress increases the cooling loads of building (Hashem Akbari et al., 1992). The reduction in the sensible heat flux may be related to the ESP as it causes citizens to consume less energy when using air conditioners (Zhang et al., 2014). Equation 14 was used to calculate ESP, and was obtained from Xu et al. (2019) and Zhang et al. (2014).

$$ESP_i (\text{kWh}) = \rho \times COP \times CC_i (W/m^2) \times Area (m^2) \quad (\text{Eq. 14})$$

where  $\rho$  represents the transformation coefficient for the conversion of heat into electrical energy ( $1 \text{ W/m}^2 = 3600 \text{ J/m}^2/\text{hour} = 1000.8 \times 10^{-6} \text{ kWh/m}^2$ ),  $COP$  is the coefficient of performance, which is the efficiency of the air-conditioner (2.9), and  $Area$  is the total area.

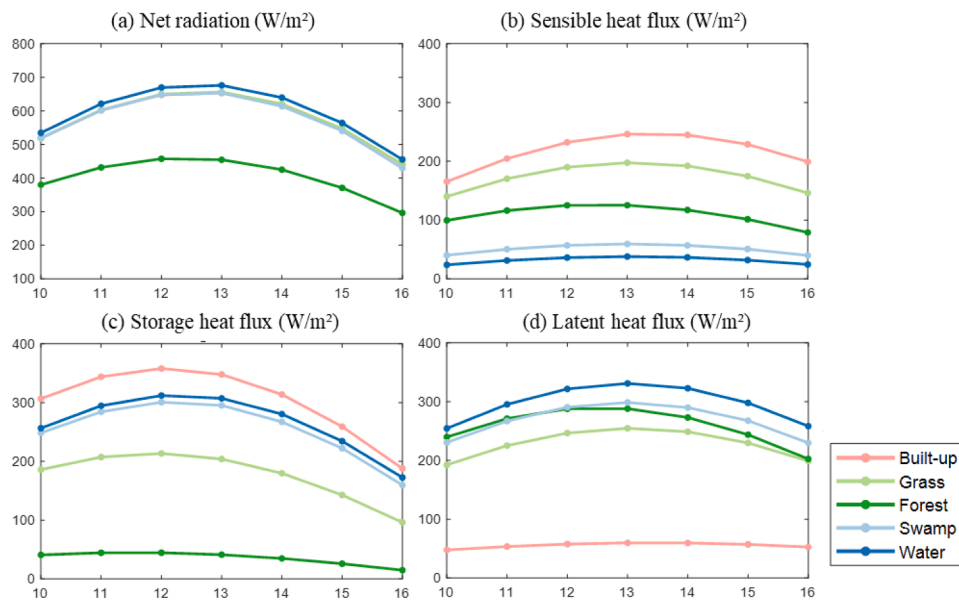


**Fig. 5.** Hourly variation (10:00 to 16:00) of energy fluxes by land-cover type. (a) Net radiation as the sum of the (b) sensible heat flux, (c) storage heat flux, and (d) latent heat flux.

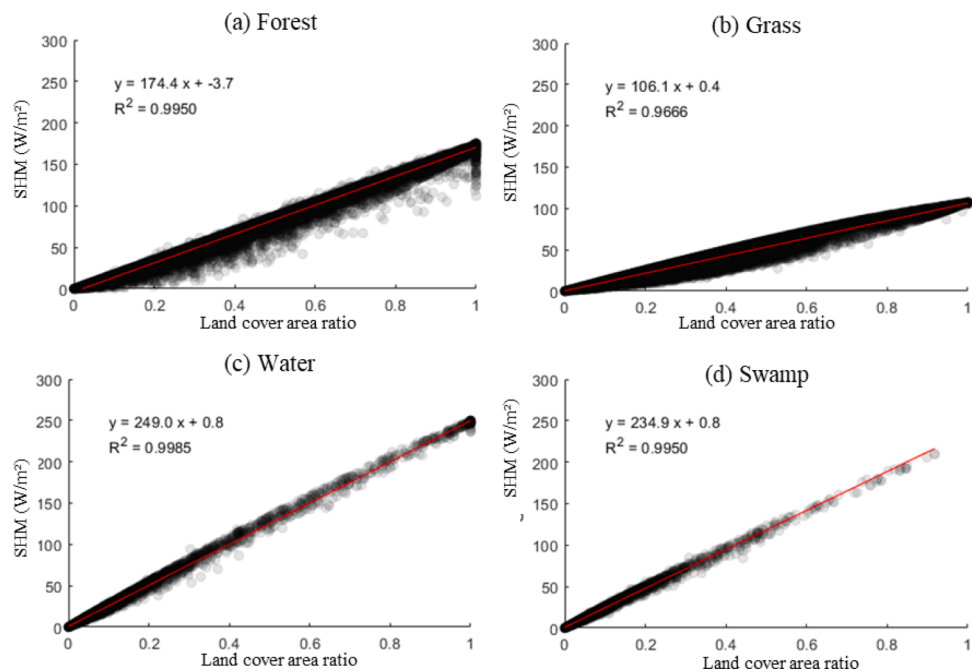


**Fig. 6.** Scatter plots (black dots) and LRM (red lines) between the land cover area ratio and SHM cooling service. .

### 3. Results

#### 3.1. Study area characteristics

The average air temperature and relative humidity during the target period were 21.2 °C and 58.5%, respectively. The air temperature increased to 28.3 °C at 15:00 and then decreased. In contrast, the relative humidity decreased to 54.2% until 15:00. Fig. 3 shows the spatial distributions of the input variables. The average forest area ratio in Yongin-si was 0.49, while that of the urban area was 0.17, indicating that the forest area was concentrated in rural areas. The average water and swamp area ratios were 0.02 and 0.01, respectively, for both Yongin-si and the urban area. The average grassland area ratios in

Yongin-si and the urban areas were 0.15 and 0.19, respectively. The opposite results were observed for the forest area (0.49 and 0.17 for Yongin-si and the urban area, respectively). The mean SVF values, with a larger values indicating a greater amount of open area, for Yongin-si and the urban area were 0.97 and 0.92, respectively, as buildings decrease the openness of urban areas. The average building ratio in Yongin-si was 0.01, while that in the urban area was 0.03. The mean albedo in Yongin-si was 0.05, which was lower than that of the urban area (0.11) as water bodies and forest areas had lower albedo than built-up areas in the study site.

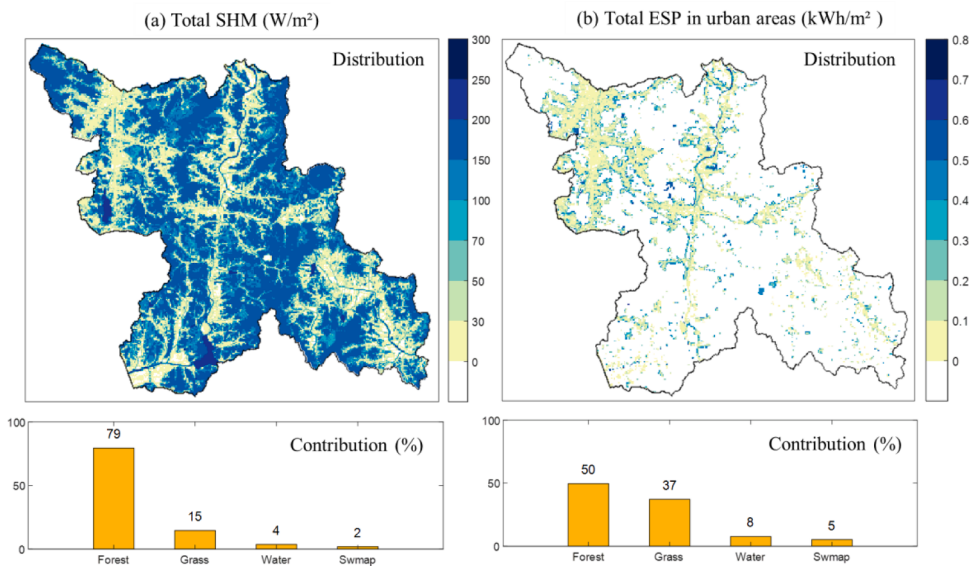


**Fig. 7.** Cooling service distribution and ecosystem cooling service contributions: (a) SHM for Yongin-si and (b) ESP for urban areas. Average cooling service during 10:00–16:00. Bar plots indicate the fraction of the cooling service attributed to each ecosystem.

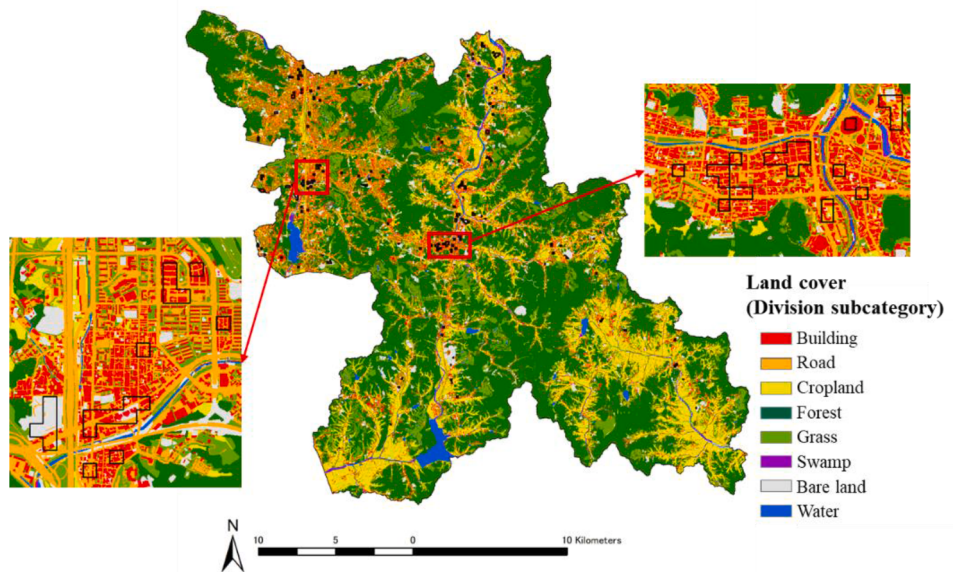


**Fig. 8.** Areas ( $100 \times 100\text{-m}$  grids) requiring ecosystem-based planning and their land-cover types.

### 3.2. Sensible heat flux by land-cover type

The simulated sensible heat flux agreed with that of previous studies (Fig. 4). The  $R^2$  values for the sensible heat flux and Bowen ratio were 0.86 and 0.81, respectively. The simulated results agreed with those of prior studies across all land cover types, i.e., built-up, forest, grass, water, crop, and swamp land. Therefore, the sensible heat flux model simulated reasonable values according to the land-cover type.

The hourly simulated heat fluxes of the five land-cover types agreed with those of previous studies (Grimmond, 1992; Ngao et al., 2015; Ryu et al., 2016; Zuo et al., 2016). First, for the built-up area (sum of road and building areas), the storage heat flux increased until 12:00 and then decreased, indicating a faster change than that of the sensible heat flux (Grimmond, 1992; Offerle et al., 2005). Although the built-up area exhibited the highest sensible heat flux (approximately  $250 \text{ W}/\text{m}^2$ ), it exhibited the lowest latent heat flux (approximately  $60 \text{ W}/\text{m}^2$ ), which is similar to the results obtained by Ryu et al. (2016). For the grass area,

the maximum latent heat flux from evapotranspiration was approximately  $250 \text{ W}/\text{m}^2$  at 13:00, and the hourly variation and peak value were similar to those of Ngao et al. (2015) (maximum latent heat flux ranged from  $183$  to  $284 \text{ W}/\text{m}^2$ ). Zuo et al. (2016) observed the latent heat flux of water surfaces ( $360$ – $770 \text{ W}/\text{m}^2$ ) using evaporation pans and found that it varied according to the surface temperature, moisture level, and albedo. Our result (maximum  $330 \text{ W}/\text{m}^2$ ) is similar to their observed value in moist areas (arid areas exhibited large latent heat fluxes).

The energy flux comparison by land-cover type demonstrates that the most vital ecosystem cooling service mechanism was the generation of the latent heat flux from evaporation (four ecosystems) and transpiration (forest and grassland).

### 3.3. Cooling service

#### 3.3.1. SHM by ecosystem

All four ecosystems provide SHM services, which increase when the land cover area ratio increases (Fig. 6). Each ecosystem exhibited a linear relationship with SHM, indicating that the greater the number of ecosystems, the more cooling services are provided in cities. The slope of the linear regression model (LRM) indicates the extent to which the cooling effect increases when 0.01 km<sup>2</sup> of an ecosystem is added to a grid (100%). Among the four ecosystems, water bodies exhibited the highest LRM slope. When the water area ratio increased by 0.1 in a grid, the sensible heat flux decreased by approximately 25 W/m<sup>2</sup>. The effect of swamps was similar to that of water. For forests, increasing the area ratio by 0.1 decreased the sensible heat flux by 17 W/m<sup>2</sup>. Grassland exhibited the lowest SHM and could decrease the sensible heat by 10 W/m<sup>2</sup> when increasing the area ratio by 0.1.

We also plotted the land-cover area ratio and sensible heat flux (Appendix B), and compared the results to those of previous studies that used the LST to determine ecosystem cooling effects. Fig B1 demonstrates that our results are consistent with the relationship between the land-cover ratio and LST (Hou & Estoque, 2020; Tan et al., 2021).

#### 3.3.2. Mapping SHM and ESP

The distributions of the mean SHM during 10:00–16:00 are presented in Fig. 7a, which varied according to the land-cover type. The mean SHM of all ecosystems reached 250 W/m<sup>2</sup>. The maximum SHM varied from 197 (10:00) to 282 (13:00) W/m<sup>2</sup> during the hottest period (10:00–13:00). This SHM was predominantly attributed to forests (79%), followed by grassland (15%), water bodies (4%), and swamps (2%) (Fig. 7a). The widely distributed forests surrounding the urban area provided SHM of up to 176 W/m<sup>2</sup>. Forests provided more cooling services than grassland (maximum 108 W/m<sup>2</sup>); however, the effect of grassland could still be observed in urban areas. While water bodies and swamps formed an extremely small percentage of the site area, they provided SHM services of up to 250 and 210 W/m<sup>2</sup>, respectively. This contribution ratio did not change substantially over time; however, the contribution of forests increased slightly (from 77% to 81%) between 10:00 and 16:00, while that of grassland decreased slightly (from 16% to 14%), because the difference in the sensible heat flux between forests and grassland slightly increased over time (Fig. 5b).

We determined the ESP for an urban area where people use air-conditioning (Fig. 7b). The air-conditioning energy could be reduced by an average of approximately 0.15 kWh/m<sup>2</sup> throughout the urban area, indicating that a total of  $2.2 \times 10^7$  kWh energy can be conserved during the hottest time of day (10:00–16:00); maximum of  $2.5 \times 10^7$  kWh at 14:00. The peak ESP value in the urban area was 0.19 kWh/m<sup>2</sup> at 14:00. This result was similar to that of research conducted in Beijing. Zhang et al. (2014) reported that the energy savings per unit of green space in a central urban area were below 0.2 kWh/m<sup>2</sup> in Beijing.

The average ESP was attributed to forests (50%), grassland (37%), water bodies (8%), and swamps (5%). The cooling services provided by forests in urban areas were lower than those in suburban areas; however, forests provided higher services than grassland, water bodies, and swamps. Although the forest area ratio (17%) was lower than the grassland area ratio (19%), the contribution of forests was highest in urban areas due to their shading and evapotranspiration effects. The impacts of forest, grassland, water bodies, and swamp on the ESP in the urban area were as follows:  $1.1 \times 10^7$ ,  $7.6 \times 10^6$ ,  $1.9 \times 10^6$ , and  $1.3 \times 10^6$  kWh, respectively.

## 4. Discussion

### 4.1. Most effective ecosystems for cooling

With the same area ratio, the most powerful ecosystems for cooling were water bodies and swamps (Fig. 6). The LSTs of reservoirs and lakes

larger than 2 km<sup>2</sup> were 3–4 °C lower than those of built-up areas (Chen et al., 2014), while small pond ecosystems could reduce the air temperature by up to 2.6 °C during the hottest time of the day (Syafii et al., 2016). In this study, we found that water bodies provided powerful cooling services due to their capacity for storage heat (Fig. 5c) and latent heat (high moisture status) production through evaporation (Fig. 5d).

Considering the area ratio of the study site, forest and grassland more significantly reduced the sensible heat flux than water bodies or swamps (Fig. 7). Additionally, while the area ratio of the forest land cover type was lower than that of grassland, it reduced the sensible heat flux to a greater extent. Air temperature simulation research revealed that grass cover could reduce the temperature by 1.1 °C more than asphalt surfaces (Lee et al., 2016). Forests have a greater cooling effect than grass areas due to their higher evapotranspiration rates (Douglas et al., 2009) and shading effect, which reduced downward shortwave radiation (Wang et al., 2016). In arid areas, grass can only reduce the air temperature by 2.4 °C, while trees can reduce the temperature by 5.5 °C (Wang et al., 2016) during the daytime. Therefore, the results demonstrate that forests more effectively mitigate sensible heat and improve the ESP than grassland.

### 4.2. Benefits of the proposed method based on urban energy balance

Many previous studies determined the cooling effects of water bodies or green areas by measuring the LST or air temperature (Du et al., 2016; Sun et al., 2012; Sun & Chen, 2012; Syafii et al., 2016; Wu & Zhang, 2019). LST measurement via remote sensing is particularly useful for identifying the cooling effect at the city-scale according to the land area ratio. However, it is limited by low temporal resolutions and a lack of data records (Yu et al., 2020). The sensible heat flux can be calculated for any time period with meteorological data from AWSs, building data, and land-cover information. Our method is comparable to the LST method as we can also detect the city-wide cooling effect and its changes according to land-cover area changes (Appendix B). Therefore, this study can overcome the temporal limitation of the LST method while determining the cooling services of large areas. Additionally, the results were quantified using an urban energy balance model, which allowed us to directly compare them to the cooling service results of other regions.

This study had certain limitations in cooling service calculation that should be improved upon in future studies. First, we compared the cooling services of various ecosystems at the study site using the sensible heat flux; however, this cooling service did not include the combined effects of ecosystems. When there are several ecosystems in the same area, they can cause higher (synergy effect) or lower (trade-off effect) combined cooling services than those obtained by adding the individual cooling capacities (Park et al., 2020). To analyze the combined effect, the sensible heat fluxes in the absence of the other ecosystems and combined ecosystems can be compared. Second, the implementation or maintenance costs for ecosystems were not considered when we determined the efficiency of the ecosystem cooling services. Although swamps exhibited the lowest LRM slope, their cost-effectiveness may be lower than those of other ecosystems if their costs are high. However, the combined effects and costs may differ depending on the conditions at the target site.

### 4.3. Ecosystem-service-based urban planning

Ecosystem-based urban planning is a sustainable development method as it balances human well-being with ecological maintenance (Martinez-Harms & Balvanera, 2012). Additionally, this nature-based solution provides multiple functions: regulating ecosystem services (such as climate, hydrological cycles, and water quality regulation) (Martinez-Harms & Balvanera, 2012; Meerow, 2019), and reducing inequality by providing social co-benefits (Darrel Jenerette et al., 2011). Scientific assessment is required for ecosystem-based planning and policy; therefore, quantifying and mapping ecosystem services with

appropriate spatial scales can assist in decision-making (Perrings et al., 2011).

Mapping and quantifying ecosystem services have several advantages and applications for land management systems. First, identifying the spatial distribution of cooling services informs decision-makers of area where ecosystems should be renovated (Martinez-Harms & Balvanera, 2012) and the potential benefits. For example, urban areas with no cooling services and the top 10% sensible heat flux can be considered as potential areas for renovation (Fig. 8). Based on these criteria, we selected an area of 1.9 km<sup>2</sup> with building, road, and bare land. Second, quantifying the effects of renovation allows decision-makers to predict the potential benefits of ecosystem-based planning. For example, planting trees in 5% of our selected area could reduce the sensible heat flux by 8 W/m<sup>2</sup>, leading to an ESP of 232 kWh based on our analysis. Creating water bodies or swamps of the same area can reduce the sensible heat flux by approximately 17 W/m<sup>2</sup> and save 493 kWh during the hottest period. Urban planners prefer to make decisions based on the quantitative benefit and prioritized area, integrating environmental consideration with policies (Davies et al., 2017). The proposed method can be integrated into both urban planning systems and environmental impact assessments.

Increasing ecosystem services (such as planting trees in 5% of an area) in high-density built areas is difficult. Previous studies have suggested utilizing small-scale green infrastructure, such as street trees (Park et al., 2019; Vailshery et al., 2013), green roofs and green walls (Alexandri & Jones, 2008; Morille et al., 2016; Smith & Roebber, 2011; Zöllch et al., 2016), and pocket gardens (Lin et al., 2017; Park et al., 2017), to improve sustainability and urban resilience. Water bodies and swamps are more effective than green spaces in providing ecosystem services; however, they are more difficult to construct than the latter. Introducing small-scale water bodies, such as ponds and, small low-impact development infrastructures, such as rain gardens, may resolve this issue.

Mapping is a convenient tool for monitoring ecosystem changes over time, and monitoring is critical for mid- to long-term ES preservation. Li et al. (2016) observed ecosystem service values over 20 years and found that the spatial distribution of ecosystem service hotspots changed. This study concluded that mapping can improve future long-term ES monitoring systems.

## Appendix A. Data for comparing simulated sensible heat flux and Bowen ratio

We compared the simulated sensible heat flux and Bowen ratio with those of previous studies. We selected three studies (Douglas et al., 2009; Kuang et al., 2014, 2017) that provided the date, time, and land-cover characteristics. For the sensible heat flux, we used the ten points from Kuang et al. (2014) (Table A1 1.1–1.10) and eight points from Kuang et al. (2017) (Table A1 2.1–2.8). Because they did not divide the built-up area into road and building land cover types, we assumed that half of the built-up areas were roads and half were buildings. The simulated day and time were 254th day of year (DOY) and 11:00 local solar time (LST) for Kuang et al. (2014) and 198th DOY and 10:30 LST for Kuang et al. (2017). We compared our simulated Bowen ratio with that of Kuang et al. (2014) and Douglas et al. (2009). Douglas et al. (2009) determined the Bowen ratios of forest, grass, swamp, and water areas, and the land cover data of these ten points are described in Table A1 3.1–3.10. The simulated date and time were the 217th DOY and 10:00, matching those of the Douglas et al. (2009) results.

## 5. Conclusions

Mapping the quantified cooling services of multiple ecosystems can be used to develop efficient planning tools for cooling cities. We present a method for comparing the spatially heterogeneous cooling service of a city by identifying the sensible heat flux according to the urban energy balance and the amount of energy savings. The methods demonstrated reasonable results compared to previous urban heat flux studies and exhibited similar patterns to those of the LST method cooling effects. The findings indicate that our method is more useful than LST methods as it is not temporally limited. We found that increasing the area ratios of forests, grassland, water bodies, and swamps can reduce the urban sensible heat flux by decreasing the incoming shortwave radiation and increasing the latent heat flux via evapotranspiration. Water bodies provided the greatest cooling service. Introducing small water bodies or employing low-impact development strategies such as rain gardens can improve the thermal environment in areas with low cooling services. For ecosystem-based urban planning, stakeholders can first identify areas that need to be renovated and the potential benefits of the planned ecosystems. The cooling service quantification and mapping method introduced in this study can be further improved by considering the combined effect of different land-cover types and cost-effectiveness. This method can be utilized in this ecosystem-based urban planning and can aid in improving the sustainability and resilience of cities.

## Declaration of Competing Interest

The authors declare that they have no known competing financial interests or personal relationships that could have appeared to influence the work reported in this paper.

## Funding

This research was supported by the Ecosystem Services Evaluation and Pilot Mapping Project III (grant no. 2020-060) conducted by the Korea Environment Institute and funded by the Ministry of Environment.

	Built-up	Grass	Water	Swamp	Crop	Forest	Bare land
1.1	0.90	0.10	0	0	0	0	0
1.2	0.85	0.10	0	0	0	0.05	0
1.3	0.70	0.10	0	0	0	0.10	0.10
1.4	0	0.13	0	0	0	0.13	0.74
1.5	0.65	0.18	0	0	0	0.17	0
1.6	0.33	0.24	0.43	0	0	0	0
1.7	0.01	0.30	0.04	0	0.50	0.15	0
1.8	0.02	0	0	0	0.98	0	0
1.9	0	0.18	0.82	0	0	0	0
1.10	0	0	0	0	0	1	0
2.1	0.30	0.57	0	0	0	0	0.13
2.2	0.20	0.35	0.2	0	0	0	0.25

(continued on next page)

(continued)

2.3	0.47	0.34	0	0	0	0	0.19
2.4	0.85	0.09	0	0	0	0	0.06
2.5	0.82	0.11	0	0	0	0	0.07
2.6	0.80	0.18	0	0	0	0	0.02
2.7	0.81	0.1	0	0	0	0	0.09
2.8	0.38	0.55	0	0	0	0	0.07
3.1	0	0	0	0	0	1	0
3.2	0	0	0	0	0	1	0
3.3	0	0	0	0	0	1	0
3.4	0	1	0	0	0	0	0
3.5	0	0	0	1	0	0	0
3.6	0	0	0	0.95	0	0	0.05
3.7	0	0	0	0.85	0	0	0.15
3.8	0	0	1	0	0	0	0
3.9	0	0	1	0	0	0	0
3.10	0	0	1	0	0	0	0

## Appendix B. Relationship between land-cover area ratio and sensible heat flux

Fig. B1 displays the relationship between the land cover area ratio and sensible heat flux. Each land-cover type exhibited a significant relationship with the sensible heat flux when a grid size of  $100 \times 100$  m was applied. These relationships coincided with that between the land cover ratio and land surface temperature (LST) (Hou & Estoque, 2020; Tan et al., 2021). Increases in the forest, water, and swamp area ratios decreased the sensible heat flux. In particular, water and swamp exhibited strong negative relationships with the sensible heat flux. Tan et al., (2021) and Hou & Estoque (2020) found that increasing the water area ratio by 0.1 decreased the LST by  $0.4^{\circ}\text{C}$ , which was greater decrease than that of green space with trees (0.2–0.3  $^{\circ}\text{C}$ ). They also found that increasing the grass area ratio could only decrease the LST by  $0.1^{\circ}\text{C}$  or  $0^{\circ}\text{C}$  (Hou & Estoque, 2020), which was similar to our results. Increasing the grassland area ratio increased the sensible heat. However, the slope of linear regression model (LRM) of the grassland area ( $24 \text{ W/m}^2$ ) was lower than that of the built-up area ( $107 \text{ W/m}^2$ ), indicating that the grassland ecosystem provided cooling services in built-up areas.

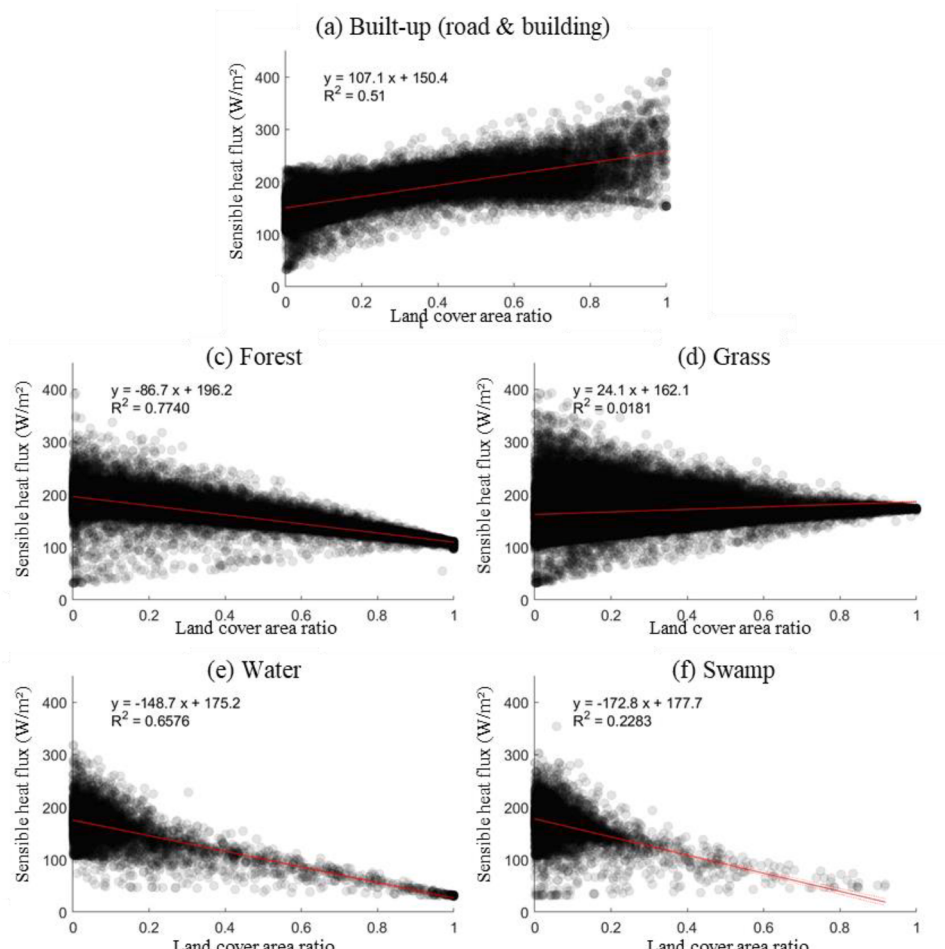


Fig. B1. Scatter plots (black dots) and LRM (red lines) between land-cover area ratio and sensible heat flux for (a) built-up, (b) forest, (c) grass, (d) water, and (e) swamp land-cover types.

## References

- Akbari, H., & Taha, H. (1992). The impact of trees and white surfaces on residential heating and cooling energy use in four Canadian cities. *Energy*, 17(2), 141–149.
- Akbari, Hashem, Davis, S., Dorsano, S., Huang, J., & Winnett, S (1992). *Cooling our communities: A guidebook on tree planting and light-colored surfacing*. Environmental Protection Agency.
- Alexandri, E., & Jones, P. (2008). Temperature decreases in an urban canyon due to green walls and green roofs in diverse climates. *Building and Environment*, 43(4), 480–493.
- Allen, R. G., Pereira, L. S., Raes, D., Smith, M., & Ab, W. (1998). *Crop evapotranspiration - Guidelines for computing crop water requirements - FAO Irrigation and drainage paper 56*. FAO. <https://doi.org/10.1016/j.eja.2010.12.001>.
- Armon, D., Rahman, M. A., & Ennos, A. R. (2013). A comparison of the shading effectiveness of five different street tree species in Manchester, UK. *Arboriculture & Urban Forestry*, 39, 157–164.
- Augusto, B., Roebeling, P., Rafael, S., Ferreira, J., Ascenso, A., & Bodilis, C. (2020). Short and medium- to long-term impacts of nature-based solutions on urban heat. *Sustainable Cities and Society*, 57, Article 102122. <https://doi.org/10.1016/j.scs.2020.102122>. February <https://doi.org/>.
- Böhner, J., & Antonić, O (2009). Land-surface parameters specific to topo-climatology. *Developments in Soil Science*, 33, 195–226. [https://doi.org/10.1016/S0166-2481\(08\)00008-1](https://doi.org/10.1016/S0166-2481(08)00008-1)
- Bolitho, A., & Miller, F. (2017). Heat as emergency, heat as chronic stress: Policy and institutional responses to vulnerability to extreme heat. *Local Environment*, 22(6), 682–698. <https://doi.org/10.1080/13549839.2016.1254169>.
- Bruse, M. (1999). Modelling and strategies for improved urban climates. *Biometeorology and urban climatology at the turn of the millennium* (p. 6). Sydney. 8–12 Novembre 1999.
- Burkhardt, B., Kroll, F., Nedkov, S., & Müller, F. (2012). Mapping ecosystem service supply, demand and budgets. *Ecological Indicators*, 21, 17–29. <https://doi.org/10.1016/j.ecolind.2011.06.019>.
- Burrough, Peter A., & McDonnell, Rachel A (1998). Spatial analysis using continuous fields. *Principles of geographical information systems* (p. 190). Oxford university press.
- Chen, Y. C., Tan, C. H., Wei, C., & Su, Z. W. (2014). Cooling effect of rivers on metropolitan Taipei using remote sensing. *International Journal of Environmental Research and Public Health*, 11(2), 1195–1210. <https://doi.org/10.3390/ijerph110201195>.
- Coutts, A. M., Tapper, N. J., Beringer, J., Loughnan, M., & Demuzere, M. (2012). Watering our cities: The capacity for Water Sensitive Urban Design to support urban cooling and improve human thermal comfort in the Australian context. *Progress in Physical Geography*, 37(1), 2–28. <https://doi.org/10.1177/030913312461032>.
- Davies, H. J., Doick, K. J., Hudson, M. D., & Schreckenberg, K. (2017). Challenges for tree officers to enhance the provision of regulating ecosystem services from urban forests. *Environmental Research*, 156, 97–107. <https://doi.org/10.1016/j.envres.2017.03.020>. February <https://doi.org/>.
- Davies, M., Steadman, P., & Oreszczyn, T. (2008). Strategies for the modification of the urban climate and the consequent impact on building energy use. *Energy Policy*, 36 (12), 4548–4551. <https://doi.org/10.1016/j.enpol.2008.09.013>.
- De Bruin, H. A. R., & Holtslag, A. A. M. (1982). A simple parameterization of the surface fluxes of sensible and latent heat during daytime compared with the Penman-Monteith concept. *Journal of Applied Meteorology*, 21(11), 1610–1621. [https://doi.org/10.1175/1520-0450\(1982\)021<1610:ASPOTS>2.0.CO;2](https://doi.org/10.1175/1520-0450(1982)021<1610:ASPOTS>2.0.CO;2).
- Douglas, E. M., Jacobs, J. M., Sumner, D. M., & Ray, R. L. (2009). A comparison of models for estimating potential evapotranspiration for Florida land cover types. *Journal of Hydrology*, 373(3–4), 366–376. <https://doi.org/10.1016/j.jhydrol.2009.04.029>.
- Du, H., Song, X., Jiang, H., Kan, Z., Wang, Z., & Cai, Y. (2016). Research on the cooling island effects of water body: A case study of Shanghai, China. *Ecological Indicators*, 67, 31–38. <https://doi.org/10.1016/j.ecolind.2016.02.040>.
- Erell, E., Pearlmutter, D., Boneh, D., & Kutieli, P. B. (2014). Effect of high-albedo materials on pedestrian heat stress in urban street canyons. *Urban Climate*, 10, 367–386. <https://doi.org/10.1016/j.ulclim.2013.10.005>.
- Foudi, S., Spadaro, J. V., Chiabai, A., Polanco-Martínez, J. M., & Neumann, M. B. (2017). The climatic dependencies of urban ecosystem services from green roofs: Threshold effects and non-linearity. *Ecosystem Services*, 24, 223–233. <https://doi.org/10.1016/j.ecoser.2017.03.004>.
- Grimmond, C. S. B. (1992). The suburban energy-balance - Methodological considerations and results for a midlatitude west-coast city under winter and spring conditions Rid A-2179-2009. *International Journal of Climatology*, 12(5), 481–497. <https://doi.org/10.1002/joc.3370120506>.
- Grimmond, C. S. B., Cleugh, H. A., & Oke, T. R. (1991). An objective urban heat storage model and its comparison with other schemes. *Atmospheric Environment*, 25(3), 311–326.
- Grimmond, C. S. B., & Oke, T. R. (1991). Evapotranspiration-interception model for urban areas. *Water Resources Research*, 27(7), 1739–1755. <https://doi.org/10.1029/91WR00557>.
- Grimmond, C. S. B., & Oke, T. R. (2002). Turbulent heat fluxes in urban areas: Observations and a local-scale urban meteorological parameterization scheme (LUMPS). *Journal of Applied Meteorology*, 41(7), 792–810. [https://doi.org/10.1175/1520-0450\(2002\)041<0792:THFIUA>2.0.CO;2](https://doi.org/10.1175/1520-0450(2002)041<0792:THFIUA>2.0.CO;2).
- Hanna, S. R., & Chang, J. C. (1992). Boundary-layer parameterizations for applied dispersion modeling over urban areas. *Boundary-Layer Meteorology*, 58(3), 229–259. <https://doi.org/10.1007/BF02033826>.
- Hou, H., & Estoque, R. C. (2020). Detecting cooling effect of landscape from composition and configuration: An urban heat island study on Hangzhou. *Urban Forestry and Urban Greening*, 53, Article 126719. <https://doi.org/10.1016/j.ufug.2020.126719>.
- Jacobs, C., Klok, L., Bruse, M., Cortesão, J., Lenzholzer, S., & Kluck, J. (2020). Are urban water bodies really cooling? *Urban Climate*, 32, Article 100607. <https://doi.org/10.1016/j.ulclim.2020.100607>. March 2019 <https://doi.org/>.
- Järvi, L., Grimmond, C. S. B., & Christen, A. (2011). The surface urban energy and water balance scheme (SUEWS): Evaluation in Los Angeles and Vancouver. *Journal of Hydrology*, 411(3–4), 219–237. <https://doi.org/10.1016/j.jhydrol.2011.10.001>.
- Jenerette, Darrel, G., Harlan, L. S., Stefanov, W. L., & Martin, C. A (2011). Ecosystem services and urban heat riskscape moderation: Water, green spaces, and social inequality in Phoenix, USA. *Ecological Applications*, 21(7), 2637–2651. <https://doi.org/10.1890/10-1493.1>.
- Kim, J. (2009). *Synergy effect only when the stigma of "Yongin = reckless development*. Yongin Newspaper. <http://www.yonginilbo.com/news/article.html?no=82620>.
- Kuang, W. H., Yang, T. R., Liu, A. L., Zhang, C., Lu, D. S., & Chi, W. F. (2017). An EcoCity model for regulating urban land cover structure and thermal environment: Taking Beijing as an example. *Science China Earth Sciences*, 60(6), 1098–1109. <https://doi.org/10.1007/s11430-016-9032-9>.
- Kuang, W., Dou, Y., Zhang, C., Chi, W., Liu, A., Liu, Y., Zhang, R., & Liu, J. (2014). Quantifying the heat flux regulation of metropolitan land use/land cover components by coupling remote sensing modeling with in situ measurement. *Journal of Geophysical Research : Atmospheres*, 113–130. <https://doi.org/10.1002/2014JD022249>. Received. <https://doi.org/>.
- Kumari, P., Kapur, S., Garg, V., & Kumar, K. (2020). Effect of surface temperature on energy consumption in a calibrated building: A case study of Delhi. *Climate*, 8(6). <https://doi.org/10.3390/CLIM060071>.
- Kwon, Y. J., Lee, D. K., & Kwon, Y. H. (2020). Is sensible heat flux useful for the assessment of thermal vulnerability in Seoul (Korea)? *International Journal of Environmental Research and Public Health*, 17(3). <https://doi.org/10.3390/ijerph17030963>.
- Kwon, Y. J., Lee, D. K., & Lee, K. (2019). Determining favourable and unfavourable thermal areas in Seoul using in-situ measurements: A preliminary step towards developing a smart city. *Energies*, 12, 12. <https://doi.org/10.3390/en1212230>.
- Lai, D., Liu, W., Gan, T., Liu, K., & Chen, Q. (2019). A review of mitigating strategies to improve the thermal environment and thermal comfort in urban outdoor spaces. *Science of the Total Environment*, 661, 337–353. <https://doi.org/10.1016/j.scitotenv.2019.01.062>.
- Lee, H., Holst, J., & Mayer, H. (2013). Modification of human-biometeorologically significant radiant flux densities by shading as local method to mitigate heat stress in summer within urban street canyons. *Advances in Meteorology*, 1–13. <https://doi.org/10.1155/2013/312572>.
- Lee, H., Mayer, H., & Chen, L. (2016). Contribution of trees and grasslands to the mitigation of human heat stress in a residential district of Freiburg, Southwest Germany. *Landscape and Urban Planning*, 148, 37–50. <https://doi.org/10.1016/j.landurbplan.2015.12.004>. October 2017 <https://doi.org/>.
- Lee, X., Goulden, M. L., Hollinger, D. Y., Barr, A., Black, T. A., Bohrer, G., Bracho, R., Drake, B., Goldstein, A., Gu, L., Katul, G., Kolb, T., Law, B. E., Margolis, H., Meyers, T., Monson, R., Munger, W., Oren, R., Paw, U. K., T., & Zhao, L. (2011). Observed increase in local cooling effect of deforestation at higher latitudes. *Nature*, 479(7373), 384–387. <https://doi.org/10.1038/nature10588>.
- Li, D., Sun, T., Liu, M., Yang, L., Wang, L., & Gao, Z. (2015). Contrasting responses of urban and rural surface energy budgets to heat waves explain synergies between urban heat islands and heat waves. *Environmental Research Letters*, 10, 10. <https://doi.org/10.1088/1748-9326/10/5/054009>.
- Li, G., Fang, C., & Wang, S. (2016). Exploring spatiotemporal changes in ecosystem-service values and hotspots in China. *Science of the Total Environment*, 545(546), 609–620. <https://doi.org/10.1016/j.scitotenv.2015.12.067>.
- Lin, P., Lau, S. S. Y., Qin, H., & Gou, Z. (2017). Effects of urban planning indicators on urban heat island: a case study of pocket parks in high-rise high-density environment. *Landscape and Urban Planning*, 168, 48–60. <https://doi.org/10.1016/j.landurbplan.2017.09.024>. October 2016 <https://doi.org/>.
- Loridan, T., Grimmond, C. S. B., Offerle, B. D., Young, D. T., Smith, T. E. L., Järvi, L., & Lindberg, F. (2011). Local-scale Urban Meteorological Parameterization Scheme (LUMPS): Longwave radiation parameterization and seasonality-related developments. *Journal of Applied Meteorology and Climatology*, 50(1), 185–202. <https://doi.org/10.1175/2010JAMC2474.1>.
- Luyssaert, S., Jammet, M., Stoy, P. C., Estel, S., Pongratz, J., Ceschia, E., Churkina, G., Don, A., Erb, K., Ferlicio, M., Gielen, B., Grünwald, T., Houghton, R. A., Klumpp, K., Knöhl, A., Kolb, T., Kuemmerle, T., Laurila, T., Lohila, A., & Dolman, A. J. (2014). Land management and land-cover change have impacts of similar magnitude on surface temperature. *Nature Climate Change*, 4(5), 389–393. <https://doi.org/10.1038/nclimate2196>.
- Martinez-Harms, M. J., & Balvanera, P. (2012). Methods for mapping ecosystem service supply: A review. *International Journal of Biodiversity Science, Ecosystem Services and Management*, 8(1–2), 17–25. <https://doi.org/10.1080/21513732.2012.663792>.
- Masoudi, M., Tan, P. Y., & Fadaei, M. (2021). The effects of land use on spatial pattern of urban green spaces and their cooling ability. *Urban Climate*, 35, Article 100743. <https://doi.org/10.1016/j.ulclim.2020.100743>. December 2020 <https://doi.org/>.
- Matthews, T. K. R., Wilby, R. L., & Murphy, C. (2017). Communicating the deadly consequences of global warming for human heat stress. *Proceedings of the National Academy of Sciences*, 114(15), 3861–3866. <https://doi.org/10.1073/pnas.1617526114>.

- Meerow, S. (2019). A green infrastructure spatial planning model for evaluating ecosystem service tradeoffs and synergies across three coastal megacities. *Environmental Research Letters*, 14, Article 014002. <https://doi.org/10.1088/1748-9326/ab502c>.
- Monteiro, M. V., Doick, K. J., Handley, P., & Peace, A. (2016). The impact of greenspace size on the extent of local nocturnal air temperature cooling in London. *Urban Forestry and Urban Greening*, 16, 160–169.
- Morille, B., Musy, M., & Malys, L. (2016). Preliminary study of the impact of urban greenery types on energy consumption of building at a district scale: Academic study on a canyon street in Nantes (France) weather conditions. *Energy and Buildings*, 114, 275–282. <https://doi.org/10.1016/j.enbuild.2015.06.030>.
- Moss, J. L., Doick, K. J., Smith, S., & Shahrestani, M. (2019). Influence of evaporative cooling by urban forests on cooling demand in cities. *Urban Forestry and Urban Greening*, 37, 65–73. <https://doi.org/10.1016/j.ufug.2018.07.023>. July 2018 <https://doi.org/>.
- Munang, R., Thiaw, I., Alverson, K., Liu, J., & Han, Z. (2013). The role of ecosystem services in climate change adaptation and disaster risk reduction. *Current Opinion in Environmental Sustainability*, 5(1), 47–52. <https://doi.org/10.1016/j.cosust.2013.02.002>.
- Nam, K.-H. (2009). Reckless development Yongin "Only aftereffects are accumulated. Donga. <https://www.donga.com/news/article/all/20010419/7678797/9>.
- Napoli, M., Massetti, L., Brandani, G., Petralli, M., & Orlandini, S. (2016). Modeling tree shade effect on urban ground surface temperature. *Journal of Environmental Quality*, 45(1), 146–156.
- Ngao, J., Améglio, T., Saudreau, M., Kastendeuch, P., Granier, A., & Najjar, G. (2015). Temporal variations of transpiration and latent heat fluxes from isolated linden crowns and lawns in a park at Strasbourg , France. In *9th International conference on urban climate - ICUC9, Jointly with 12th symposium on the urban environment*.
- Norton, B. A., Coutts, A. M., Livesley, S. J., Harris, R. J., Hunter, A. M., & Williams, N. S. G. (2015). Planning for cooler cities: A framework to prioritise green infrastructure to mitigate high temperatures in urban landscapes. *Landscape and Urban Planning*, 134, 127–138. <https://doi.org/10.1016/j.landurbplan.2014.10.018>.
- Offerle, B., Grimmond, C. S. B., & Fortuniak, K. (2005). Heat storage and anthropogenic heat flux in relation to the energy balance of a central European city centre. *International Journal of Climatology*, 25(10), 1405–1419. <https://doi.org/10.1002/joc.1198>.
- Ouyang, W., Morakinyo, T. E., Ren, C., & Ng, E. (2020). The cooling efficiency of variable greenery coverage ratios in different urban densities: A study in a subtropical climate. *Building and Environment*, 174, Article 106772. <https://doi.org/10.1016/j.buildenv.2020.106772>. February <https://doi.org/>.
- Park, C. Y., Lee, D. K., Krayenhoff, E. S., Heo, H. K., Hyun, J. H., Oh, K., & Park, T. Y. (2019). Variations in pedestrian mean radiant temperature based on the spacing and size of street trees. *Sustainable Cities and Society*, 48, 1–9. <https://doi.org/10.1016/j.scs.2019.101521>.
- Park, C. Y., Thorne, J. H., Hashimoto, S., Lee, D. K., & Takahashi, K. (2021). Differing spatial patterns of the urban heat exposure of elderly populations in two megacities identifies alternate adaptation strategies. *Science of the Total Environment*, , Article 146455. <https://doi.org/10.1016/j.scitotenv.2021.146455>.
- Park, C. Y., Yoon, E. J., Lee, D. K., & Thorne, J. H. (2020). Integrating four radiant heat load mitigation strategies is an efficient intervention to improve human health in urban environments. *Science of the Total Environment*, 698, Article 134259. <https://doi.org/10.1016/j.scitotenv.2019.134259>.
- Park, J., Kim, J. H., Lee, D. K., Park, C. Y., & Jeong, S. G. (2017). The influence of small green space type and structure at the street level on urban heat island mitigation. *Urban Forestry and Urban Greening*, 21, 203–212. <https://doi.org/10.1016/j.ufug.2016.12.005>.
- Peng, J., Liu, Q., Xu, Z., Lyu, D., Du, Y., Qiao, R., & Wu, J. (2020). How to effectively mitigate urban heat island effect? A perspective of waterbody patch size threshold. *Landscape and Urban Planning*, 202(5), Article 103873. <https://doi.org/10.1016/j.landurbplan.2020.103873>.
- Perrings, C., Duraiappah, A., Larigauderie, A., & Mooney, H. (2011). The biodiversity and ecosystem services science-policy interface. *Science*, 331(6021), 1139–1140. <https://doi.org/10.1126/science.1202400>.
- Roberts, S. M., Oke, T. R., Grimmond, C. S. B., & Voogt, J. A. (2006). Comparison of four methods to estimate urban heat storage. *Journal of Applied Meteorology and Climatology*, 45(12), 1766–1781. <https://doi.org/10.1175/JAM2432.1>.
- Ryu, Y. H., Bou-Zeid, E., Wang, Z. H., & Smith, J. A. (2016). Realistic representation of trees in an urban canopy model. *Boundary-Layer Meteorology*, 159(2), 193–220. <https://doi.org/10.1007/s10546-015-0120-y>.
- Saaroni, H., & Ziv, B. (2003). The impact of a small lake on heat stress in a Mediterranean urban park: The case of Tel Aviv, Israel. *International Journal of Biometeorology*, 47 (3), 156–165. <https://doi.org/10.1007/s00484-003-0161-7>.
- Smith, kathryn R., & Roebber, paul J (2011). Green roof mitigation potential for a proxy future climate scenario in Chicago , Illinois. *American Meteorological Society*, 26(12), 507–522. <https://doi.org/10.1175/2010JAMC2337.1>.
- Sun, R., Chen, A., Chen, L., & Lü, Y. (2012). Cooling effects of wetlands in an urban region: The case of Beijing. *Ecological Indicators*, 20, 57–64. <https://doi.org/10.1016/j.ecolind.2012.02.006>.
- Sun, R., & Chen, L. (2012). How can urban water bodies be designed for climate adaptation? *Landscape and Urban Planning*, 105(1–2), 27–33. <https://doi.org/10.1016/j.landurbplan.2011.11.018>.
- Syafii, N. I., Ichinose, M., Wong, N. H., Kumakura, E., Jusuf, S. K., & Chigusa, K. (2016). Experimental study on the influence of urban water body on thermal environment at outdoor scale model. *Procedia Engineering*, 169, 191–198. <https://doi.org/10.1016/j.proeng.2016.10.023>.
- Taha, H. (1997). Urban climates and heat islands: Albedo, evapotranspiration, and anthropogenic heat. *Energy and Buildings*, 25(2), 99–103.
- Tan, X., Sun, X., Huang, C., Yuan, Y., & Hou, D. (2021). Comparison of cooling effect between green space and water body. *Sustainable Cities and Society*, 67, Article 102711. <https://doi.org/10.1016/j.scs.2021.102711>.
- Thorsson, S., Rocklöv, J., Konarska, J., Lindberg, F., Holmer, B., Douillet, B., & Rayner, D. (2014). Mean radiant temperature - A predictor of heat related mortality. *Urban Climate*, 10, 332–345. <https://doi.org/10.1016/j.uclim.2014.01.004>.
- Vaishshery, L. S., Jagannohan, M., & Nagendra, H. (2013). Effect of street trees on microclimate and air pollution in a tropical city. *Urban Forestry & Urban Greening*, 12 (3), 408–415.
- Venevsky, S., Le Page, Y., Pereira, J. M. C., & Wu, C. (2019). Analysis fire patterns and drivers with a global SEVER-FIRE v1.0 model incorporated into dynamic global vegetation model and satellite and on-ground observations. *Geoscientific Model Development*, 12(1), 89–110. <https://doi.org/10.5194/gmd-12-89-2019>.
- Wang, Z. H., Zhao, X., Yang, J., & Song, J. (2016). Cooling and energy saving potentials of shade trees and urban lawns in a desert city. *Applied Energy*, 161, 437–444. <https://doi.org/10.1016/j.apenergy.2015.10.047>.
- Wu, Zhifeng, & Chen, L. (2017). Optimizing the spatial arrangement of trees in residential neighborhoods for better cooling effects: Integrating modeling with in-situ measurements. *Landscape and Urban Planning*, 167, 463–472. <https://doi.org/10.1016/j.landurbplan.2017.07.015>.
- Wu, Zhijie, & Zhang, Y. (2019). Water bodies' cooling effects on urban land daytime surface temperature: Ecosystem service reducing heat island effect. *Sustainability (Switzerland)*, 11(3), 1–11. <https://doi.org/10.3390/su11030787>.
- Xu, X., Liu, S., Sun, S., Zhang, W., Liu, Y., Lao, Z., Guo, G., Smith, K., Cui, Y., Liu, W., Higueras García, E., & Zhu, J. (2019). Evaluation of energy saving potential of an urban green space and its water bodies. *Energy and Buildings*, 188(189), 58–70. <https://doi.org/10.1016/j.enbuild.2019.02.003>.
- Yan, C., Guo, Q., Li, H., Li, L., & Qiu, G. Y. (2020). Quantifying the cooling effect of urban vegetation by mobile traverse method: A local-scale urban heat island study in a subtropical megacity. *Building and Environment*, 169, Article 106541. <https://doi.org/10.1016/j.buildenv.2019.106541>.
- Yu, Z., Chen, T., Yang, G., Sun, R., Xie, W., & Vejre, H. (2020). Quantifying seasonal and diurnal contributions of urban landscapes to heat energy dynamics. *Applied Energy*, 264, Article 114724. <https://doi.org/10.1016/j.apenergy.2020.114724>.
- Zardo, L., Geneletti, D., Pérez-Soba, M., & Van Epen, M. (2017). Estimating the cooling capacity of green infrastructures to support urban planning. *Ecosystem Services*, 26, 225–235. <https://doi.org/10.1016/j.ecoser.2017.06.016>.
- Zhang, B., Xie, G., di Gao, J., xi., & Yang, Y. (2014). The cooling effect of urban green spaces as a contribution to energy-saving and emission-reduction: A case study in Beijing, China. *Building and Environment*, 76, 37–43. <https://doi.org/10.1016/j.buildenv.2014.03.003>.
- Zhuang, Q., Wu, B., Yan, N., Zhu, W., & Xing, Q. (2016). A method for sensible heat flux model parameterization based on radiometric surface temperature and environmental factors without involving the parameter KB-1. *International Journal of Applied Earth Observation and Geoinformation*, 47, 50–59. <https://doi.org/10.1016/j.jag.2015.11.015>.
- Zitter, C. D., Pedersen, E. J., Kucharik, C. J., & Turner, M. G. (2019). Scale-dependent interactions between tree canopy cover and impervious surfaces reduce daytime urban heat during summer. *Proceedings of the National Academy of Sciences of the United States of America*, 116(15), 7575–7580. <https://doi.org/10.1073/pnas.1817561116>.
- Zöchl, T., Maderspacher, J., Wamsler, C., & Pauleit, S. (2016). Using green infrastructure for urban climate-proofing: An evaluation of heat mitigation measures at the micro-scale. *Urban Forestry and Urban Greening*, 20, 305–316. <https://doi.org/10.1016/j.ufug.2016.09.011>.
- Zuo, H., Chen, B., Wang, S., Guo, Y., Zuo, B., Wu, L., & Gao, X. (2016). Observational study on complementary relationship between pan evaporation and actual evapotranspiration and its variation with pan type. *Agricultural and Forest Meteorology*, 222, 1–9. <https://doi.org/10.1016/j.agrformet.2016.03.002>.